



Single-sided ultrasonic welding of carbon fiber/Nylon 66 composite

Qian Zhi¹ · Jin-Ming Ma¹ · Xin-Rong Tan¹ · Zhong-Xia Liu² · Zeng-Guo Tian² · Pei-Chung Wang³

Received: 19 November 2020 / Accepted: 8 July 2021 / Published online: 17 July 2021
© International Institute of Welding 2021

Abstract

In this study, the weldability of single-sided ultrasonic welding of 4-mm-thick carbon fiber/Nylon 66 composite was studied. Extensive welding was performed, and the weld microstructures, fractographies, and appearances of welded joints were examined and analyzed. It was found that the strengths of single-sided ultrasonic welded (SSUWed) joints made with proper welding variables are comparable to that of the ultrasonic welded joints. The solid SSUWed joints with introducing a gap of 1.0 mm can be produced with the use of double-pulse ultrasonic vibration schedule. The robust welding variables include a weld pressure of 0.17 MPa and a weld time of 1.3 s for the first vibration pulse, 5-s cooling, and a weld time of 1.3 s for the second vibration pulse. Microstructure analyses and mechanical testing of the welds revealed that the application of second ultrasonic pulse caused the melting of the materials at periphery of the existing weld, and consequently resulted in an increase in weld area. The use of the second vibration pulse not only improved the strength but also decreased the scatter in strength of the ultrasonic welded 4-mm-thick carbon fiber/Nylon 66 composite. The double-pulse vibration schedule improves the robustness of the SSUW and increases the flexibility of product designs that rely on the ultrasonic welding for assembly.

Keywords Single-sided ultrasonic welding · Carbon fiber/Nylon 66 composite · Single-sided double pulse ultrasonic welding · Weld strength · Decorative quality

Recommended for publication by Commission XVI - Polymer Joining and Adhesive Technology

✉ Xin-Rong Tan
tanxinrong0@163.com

✉ Zhong-Xia Liu
liuzhongxia0@163.com

¹ Hunan Provincial Key Laboratory of Advanced Materials for New Energy Storage and Conversion, Hunan Provincial Key Defense Laboratory of High Temperature Wear-Resisting Materials and Preparation Technology, Hunan Engineering Research Center of Forming Technology and Damage Resistance Evaluation for High Efficiency Light Alloy Components, School of Materials Science and Engineering, Hunan University of Science and Technology, Xiangtan 411201, China

² School of Physics and Engineering, Zhengzhou University, Zhengzhou 450052, China

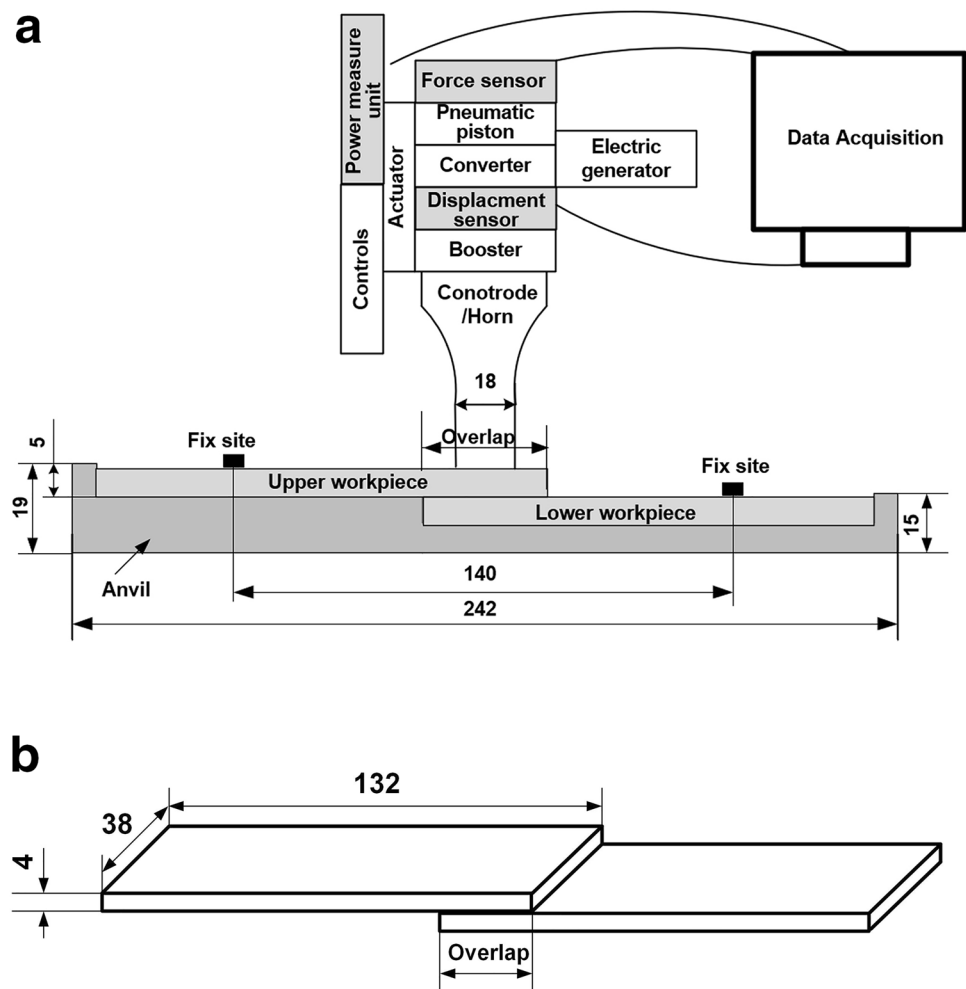
³ GM Global Technical Center, 30470 Harley Earl Boulevard, Warren, MI 48092-2031, USA

1 Introduction

Recent trends toward economically fabricating vehicle structures while ensuring structural integrity have led to the development of carbon fiber/Nylon 66 for automotive applications [1–5]. To make large and complex structures, the joining of carbon fiber/Nylon 66 composite is inevitable. Among all the available methods, ultrasonic welding is one of the most popular techniques in automotive manufacturing because it is relatively fast, economical, easily automated, and suitable for mass production [6–11]. Ultrasonic welding is a process where mechanical vibration is transmitted between the horn and anvil. Referring to Fig. 1, workpieces to be joined are placed between the horn and anvil, a clamping force is applied to the horn, and mechanical vibration passing between the horn and anvil through the workpieces. Heat is generated within the workpieces by internal damping (i.e., intermolecular friction at the joint interface), and energy dissipation is concentrated at the faying interface between the workpieces and welds the workpieces together [12, 13].

In practice, the welding of the workpieces may be constrained by part geometry and product designs. It is difficult

Fig. 1 Schematic for **a** ultrasonic welding of injection molded carbon fiber/Nylon 66 composite; **b** lap joint (dimensions in mm)



to support the lower sheet using anvil in ultrasonic welding of some particular situations. Therefore, single-sided ultrasonic welding (SSUW) is needed. In the SSUW process, the coupon is placed against the large or closed-form specimen, with the lower sheet resting upon an anvil. The welding horn is then placed against the coupons. Ultrasonic vibration is conducted through to the horn and the vibration wave transmitted through the upper sheet, and through the lower sheet to the anvil. A weld may form at the part-to-part interface due to the interfacial friction and intermolecular friction. It would be desirable to develop a single-sided ultrasonic welding process in order to facilitate formation of high-quality welds in joining of thermoplastic composites. Although there have been a number of studies devoted to ultrasonic welding of thermoplastic composites [14–19], single-sided ultrasonic welding has not been reported. To implement the molded thermoplastic composites for vehicle body structures, it is essential that

the development of single-sided ultrasonic welding process be obtained.

In this study, the weldability in single-sided ultrasonic welding of lapped carbon fiber/Nylon 66 composite with 30% mass fiber is studied. First, the effect of process variables (e.g., weld time, weld pressure, overlap distance, and gap between the workpieces) on the strength and microstructures of the welds are examined. To improve the process robustness, a single-sided ultrasonic welding with double-pulse schedule is proposed and evaluated. Test results of the SSUWed and single-sided double pulse ultrasonic welded joints are compared and joining mechanism of single-sided double pulse ultrasonic welded joints is analyzed. Finally, the effect of single-sided double pulse ultrasonic welding (SSDPW) on the surface quality of the joints is discussed. This study provides a method to improve the robustness of the single-sided ultrasonic welding and increase the flexibility of product designs that rely on the ultrasonic welding for assembly.

2 Experimental procedure

2.1 Injection molding carbon fiber-reinforced composite

Commercial Nylon 66 and carbon fiber (24 K, T300 type, Toray Carbon Magic Co. Ltd.) with a length of 2 mm were selected in this study. Carbon fibers were first cleaned with a concentrated solution of nitric acid and then surface pretreated using 8% diglycidyl ether of bisphenol solution in acetone. Both Nylon 66 and pretreated carbon fibers were dried at 80 °C under vacuum condition for 3 h before being used to fabricate carbon fiber/Nylon 66 composite with 30% mass.

A twin-screw extruder with two separate inlets was used to mold carbon fiber/Nylon 66 composite. Nylon 66 was added in the first hopper while carbon fibers were added into the second hopper. To minimize the fracture of carbon fiber during compounding, Nylon 66 was fully melted before carbon fibers were added. The processing temperatures were 270~280 °C and the screw speed was 180 rpm. After fully mixing Nylon 66 with carbon fibers in a twin-screw extruder, carbon fiber/Nylon 66 composite were processed into the pellets with a length of 2 mm. The pellets were then fed into the injection extruder to mold into the coupons with the dimensions of 4.0 mm × 38 mm × 132 mm. The mechanical properties of the injection-molded carbon fiber/Nylon 66 composite were measured and the results are shown in Table 1.

Table 1 Mechanical properties of molded 4-mm-thick carbon fiber/Nylon 66 composite coupons with 30% mass carbon fiber

	Tensile strength (MPa)	Std. dev. (MPa)	Elastic modulus (MPa)	Std. dev. (MPa)
Nylon66	78	2	2901	210
Carbon fiber/Nylon 66 composite	99.2	3	8936	421

2.2 Ultrasonic welding process

Ultrasonic welding process was performed using the KZH-2026 multi-function ultrasonic welding machine (Weihai Kaizheng Ultrasonic Technologies Co. Ltd., China) with a nominal power of 2.6 kW and a nominal frequency of 20 kHz. The machine includes three welding modes, namely energy mode, time mode, and horn-displacement mode. The value of the weld energy for energy mode, the weld time for time mode, and the horn displacement for horn-displacement mode are preset prior to welding to control the welding process. The workpieces were then welded using nominal power of the machine. The machine was also equipped with a data acquisition system that combined with pressure sensor, horn-displacement sensor and timer were integrated in the controller of the ultrasonic welding machine. While the weld pressure, weld energy and displacement of horn were recorded online in personal computer as a function of time by the data acquisition system. The welding setups used in this study are schematically shown in Figs. 1 and 2. Figure 1 shows the normal ultrasonic welding (UW) and Fig. 2 schematically illustrates single-sided ultrasonic welding with single-lap shear configuration specimen.

Different from the UW, a gap of 2 mm was spaced between the bottom surface of the lower workpiece and anvil in the SSUW. Two small support blocks about 2.5 mm in width were put at both ends of the gap, and thus a suspension distance of 25 mm was obtained as shown in Fig. 2a (the dimensions of the gap and block were according to the actual automobile production). To simulate the effect of the gap between workpieces on the joint strength, gaps between upper and lower workpieces were created by introducing shims with various thicknesses. For single-sided ultrasonic welding, the weld time mode was selected and the values of the weld time, weld pressure, and hold time were preset prior to welding and then ultrasonic welding was performed using nominal power. When the weld time approached to the preset value, the ultrasonic wave oscillation was stopped and the coupons were held for 3.0 s to solidify the molten material. All specimens were welded using a 7075 aluminum horn

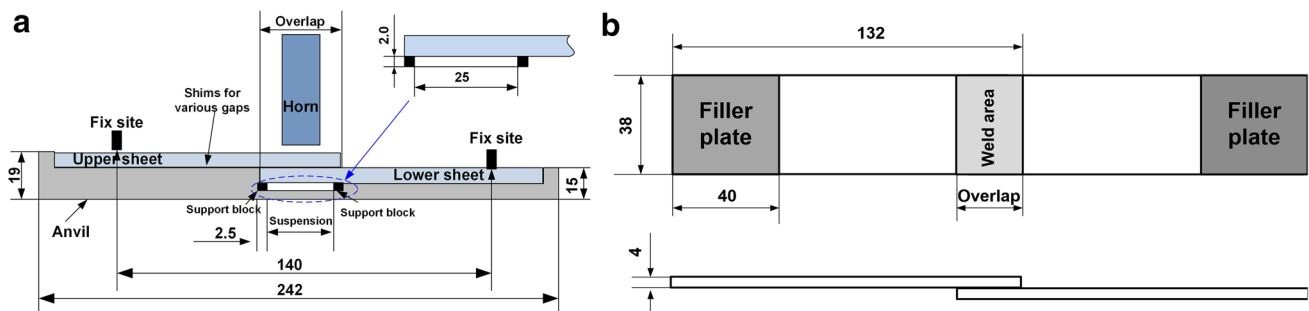


Fig. 2 Schematic of **a** single-sided ultrasonic welding; **b** a lap-shear specimen (dimensions in mm)

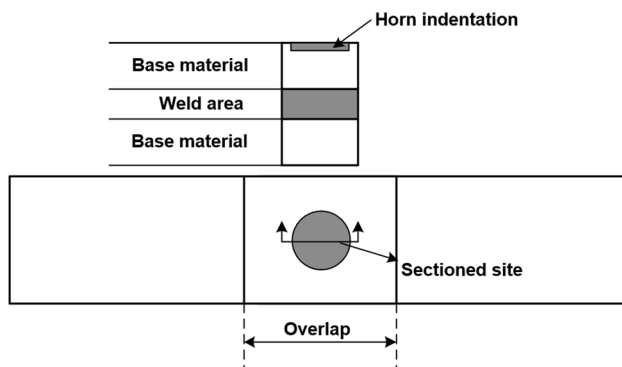


Fig. 3 Schematic of sample preparation for examining the microstructure of the ultrasonic welded 4-mm-thick carbon fiber/Nylon 66 composite

with diameter of 18 mm and three replicates were welded per condition. Weld size and weld strength are used as an indicator for weld quality. The actual weld size was estimated by measuring the area of the weld after mechanical tests. The weld area and strength were determined by the average value of three replicates for each welding condition.

2.3 Weld microstructure

To assess the characteristics of the weld microstructure of the ultrasonic welded joints, the specimens were prepared using the procedures shown in Fig. 3 for the tested joints. Referring to Fig. 3, the joints were notched from the central position of the weld. Then, the pre-notched specimens were immersed in liquid nitrogen for 10 min. The embrittled specimens were broken off from the notched site; the broken specimens were sputter-coated with gold for 50 s, and the microstructures of the welds were examined with scanning electron microscope (JSM6700F, JEOL).

2.4 Quasi-static test

Quasi-static tests were performed by loading each specimen to failure in an MTS 810 (MTS Systems Corporation) tensile

Fig. 4 Effect of process variables on the SSUWed carbon fiber/Nylon 66 composite joints with an overlap distance of 30 mm: **a** strength; **b** weld area

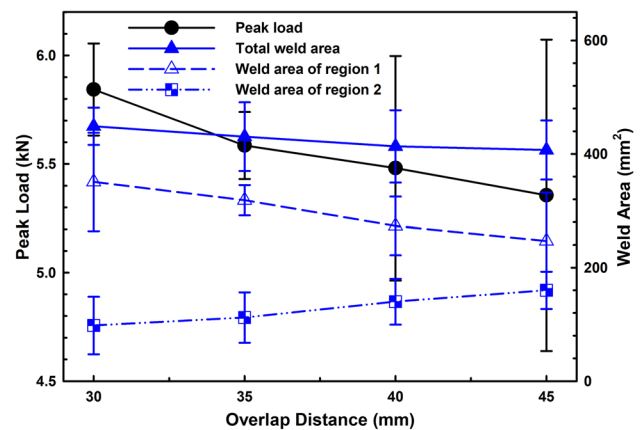
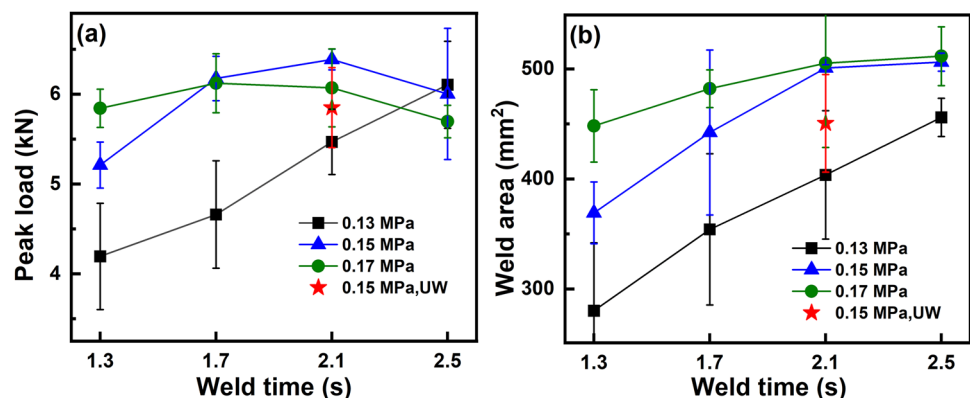


Fig. 5 Effect of overlap distance on the strength and weld area of the SSUWed carbon fiber/Nylon 66 composite

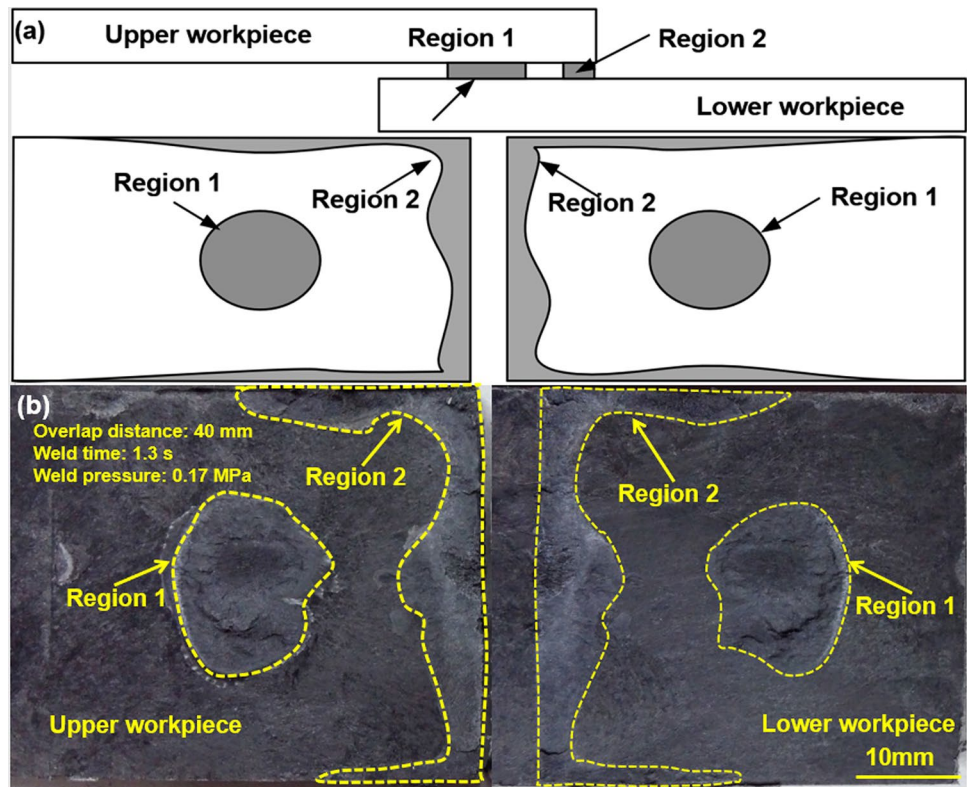
tester according to ASTM D1002-2001. To minimize the bending stresses inherent in the testing of single-lap weld specimens, filler plates shown in Fig. 2b were attached to both ends of the specimen using masking tape to accommodate the sample offset. Load vs. displacement results were obtained, as the specimens were loaded at a stroke rate of 2.0 mm/min. The performance of the joint was evaluated by the peak load. Three replicates were performed, and the average peak loads were reported.

3 Results and discussion

3.1 Effect of process variables on strength of SSUW joints

To evaluate the weldability in SSUW of 4-mm-thick carbon fiber/Nylon 66 composite with 30% mass fiber, extensive welding tests were performed. Figure 4 shows the effect of process parameters on the strength and weld area of the SSUWed carbon fiber/Nylon 66 composite with an overlap distance of 30 mm. For the purpose of comparison, the strength and weld area of the UWEd joints made

Fig. 6 Fracture surfaces of SSUWed carbon fiber/Nylon 66 composite joints made with an overlap distance of 40 mm: **a** schematic of the fracture surface; **b** fracture surface



with an overlap distance of 30 mm under a weld time of 2.1 s and a weld pressure of 0.15 MPa [9] are also included in Fig. 4. As shown, the peak loads of the SSUWed joints which welded with 2.1 s are higher than that of the UWed welds. Examinations of the fractured joints revealed that this characteristic was primarily attributed to the intimate contacts of the workpieces under the weld pressures (i.e., 0.15 MPa and 0.17 MPa). This observation was supported by the weld area results shown in Fig. 4b where the weld areas of the SSUW joints made with 0.15 MPa and 0.17 MPa

were larger than that of the ultrasonic welds supporting the above observations.

Further examination of the results shown in Fig. 4 indicated that while the strengths of the SSUWed joints made with the weld pressures of 0.13 MPa and 0.15 MPa increased with an increase in weld area, the strengths of the SSUWed joints made with a weld pressure of 0.17 MPa were influenced slightly by the weld area. This difference was likely attributed to the reduction in thickness of the melt resulting from the joints made with large weld pressure. Previous studies showed that the strength of the joints depended upon the area and melt thickness of a weld [20–24]. The positive effect from an increase in weld area was likely cancelled out by the negative impact from the reduction in melt thickness for the joints made with a weld pressure of 0.17 MPa, and consequently the strengths of the joints were changed little by an increase in weld area.

Referring to Fig. 4, significant scatter in joint strength was observed for the SSUW welds made with a weld pressure of 0.13 MPa. Careful examination of the tested joints indicated that the workpieces were not in intimate contacts under a low weld pressure, and consequently affected the mechanical vibration transmitting through the workpieces. To understand how the contact of the workpieces affects the ultrasonic welding of carbon fiber-reinforced composite, the effect of gap between the workpieces on the strength of the SSUW welds was examined and the results will be discussed later.

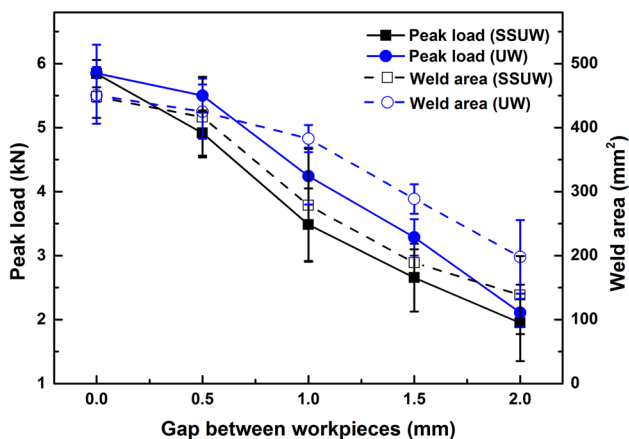


Fig. 7 Effect of gap between the workpieces on the strength of the SSUWed and UWed carbon fiber/Nylon 66 composites made with an overlap distance of 30 mm

Fig. 8 Failure modes for SSUWed carbon fiber/Nylon 66 composite with/without gap between the workpieces with an overlap distance of 40 mm under a weld pressure of 0.17 MPa and a weld time of 1.3 s: **a** failure through the workpieces for the joints; **b** interfacial failure for the joints made with a gap of 1.0 mm

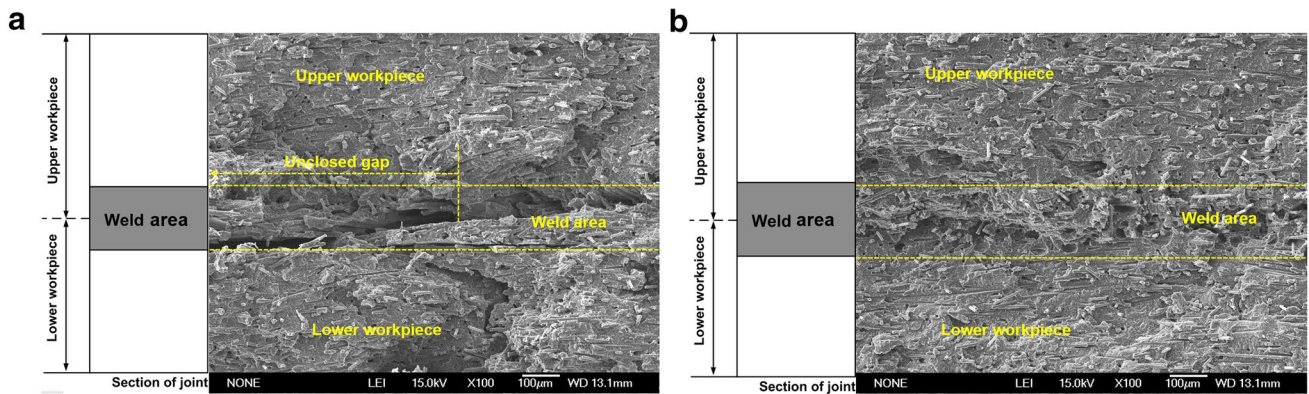
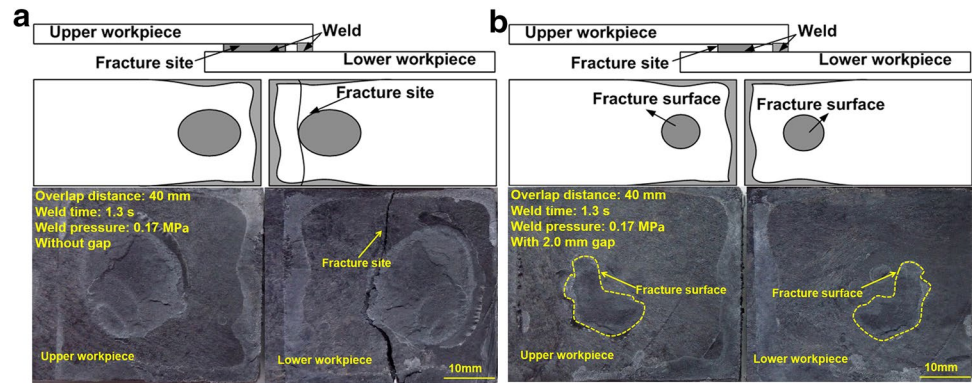


Fig. 9 Microstructures of the SSUWed carbon fiber/Nylon 66 composite with an overlap distance of 40 mm under a weld pressure of 0.17 MPa and a weld time of 1.3 s: **a** a nominal weld, **b** a weld with a gap of 1.0 mm between the workpieces

3.2 Effect of overlap distance on joint strength

Since the weld pitch affects the heat generation in ultrasonic welding of thermoplastic composite [9, 25], the

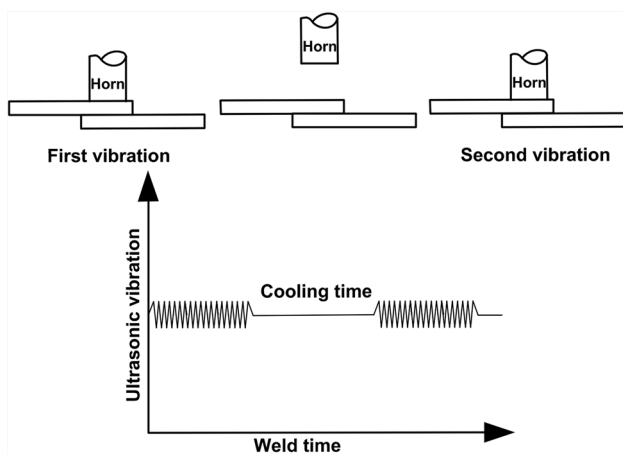


Fig. 10 Single-sided double-pulse ultrasonic welding of carbon fiber/Nylon 66 composite with 30% mass

effect of overlap distance (i.e., weld pitch) on the strength of the SSUW joints was examined. Lap joints with various overlap distances were fabricated and mechanically tested. Figure 5 presents the effect of overlap distance on the strengths and weld areas of the SSUW joints. The typical weld area of a joint is shown in Fig. 6 and it was clearly that the weld area contained two regions, namely, region 1 (the middle of the overlap region) and region 2 (edges of the overlap). Referring to Fig. 5, the strength of the SSUW joints decreased as the overlap distance increased. Careful observations of the results showed that the strengths of the SSUW joints were closely related to the weld area of region 1 instead of the total weld area or the weld area of region 2. This characteristic was mainly because that a high stress raiser was developed around the notch of the weld at the region 1 under an applied loading. As the overlap distance increased, the weld area in the middle of the overlap region decreased as shown in Fig. 5, and consequently led to a high stress at the periphery of the region 1. This high stress raiser resulted in a decrease in strength of the SSUW joints.

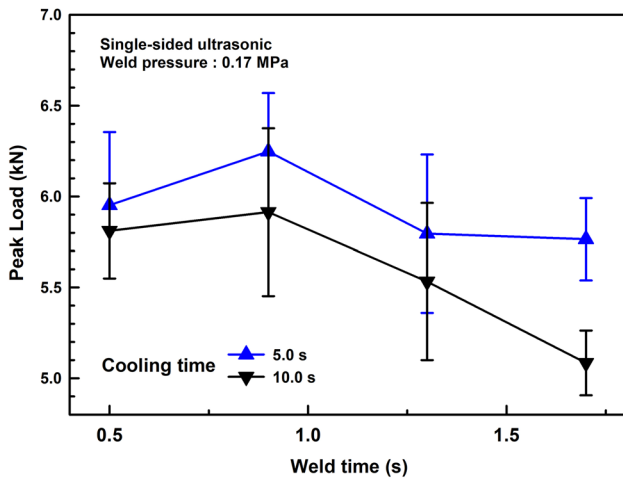


Fig. 11 Effect of cooling time between two pulses on the strength of the SSDPUWed carbon fiber/Nylon 66 composite with an overlap distance of 40 mm

3.3 Effect of gap between the workpieces on joint strength

Since carbon fiber-reinforced composite were injection molded, it is inevitable that the workpieces may have variations in dimensions. Furthermore, the workpieces may have some distortion at the clamping position. These variations could influence the contacts of the workpieces and introduce a gap at faying interface, and hence affect the transmission of the mechanical vibrations through the workpieces. To examine the effect of gap on the strength of the SSUWed joints, the joints were made with the introduction of various gaps (i.e., 0.5, 1.0, 1.5, and 2.0 mm) between the workpieces, and an

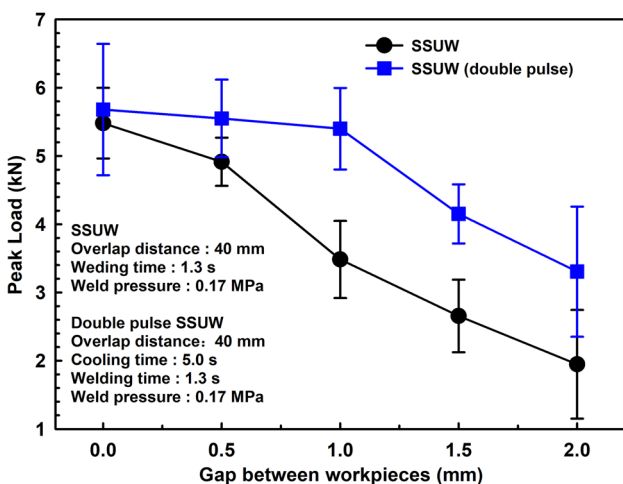


Fig. 12 Effect of gap on the strengths of single-sided and single-sided double-pulse ultrasonic welding of carbon fiber/Nylon 66 composite with an overlap distance of 40 mm

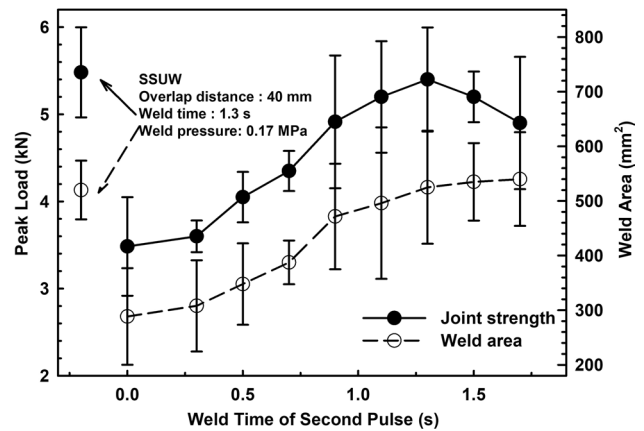


Fig. 13 Effect of weld time of the second pulse on the strength and weld area in SSDPUWed carbon fiber/Nylon 66 composite with a gap of 1.0 mm and an overlap distance of 40 mm

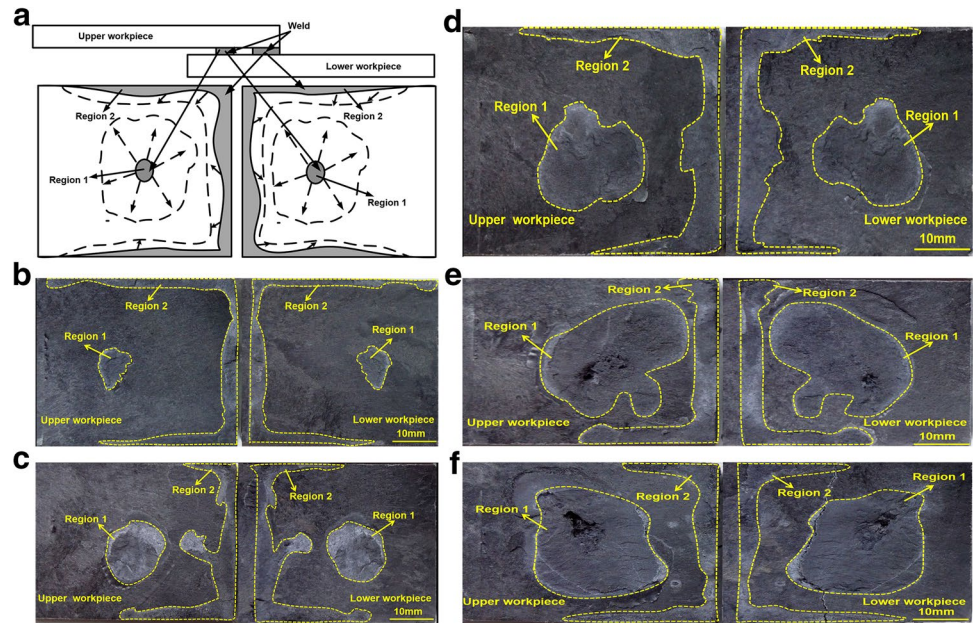
overlap distance of 30 mm. Figure 7 presents the effect of gap on the strengths of the SSUW 4-mm-thick carbon fiber/Nylon 66 composite. For the purpose of comparison, the effect of gap on the strength of the ultrasonic welds was examined and the results are included in Fig. 7. As can be observed in Fig. 7, the strengths of both SSUWed and UWed joints decreased with an increase in gap between the workpieces.

Referring to Fig. 7, the weld areas of the UWed joints were larger than that of the SSUWed joints. This was primarily caused by the difference in contact conditions between these two welding processes. Because the workpieces were not supported by the anvil for SSUW, the workpieces likely were not in intimate contacts under a given weld pressure, and therefore the mechanical vibrations were not transmitted properly through the workpieces. As a result, heat generated within the workpieces by internal damping was reduced, and consequently it led to a decrease in weld area.

3.4 Failure modes of single-sided ultrasonic welded joints

Once we examined the effects of process and geometry variables on the joint strengths, the failure modes of the tested SSUW joints were analyzed next. Visual examinations of fractured joints indicated that the joints with various overlap distances and gaps between workpieces had similar failure modes, and therefore the joints with an overlap distance of 40 mm were selected. Figure 8a and b present the workpiece failure and interfacial failure of the joints, respectively. Referring to Fig. 8, while the workpiece failure was observed for the nominal joints having the weld area greater than ~490 mm², the interfacial fracture became dominant for the undersized welds.

Fig. 14 Effect of weld time of the second pulse on the growth of single-sided double-pulse ultrasonic welds: **a** schematic of the weld growth, **b** area of a single-sided weld with a gap of 1.0 mm, **c** area of the weld growth of single-sided double-pulse weld with weld time of 0.5 s, **d** 0.9 s, **e** 1.3 s, and **f** 1.7 s



To further examine the failure mode, the microstructures of joint with the workpiece failure shown in Fig. 8a and a joint with the interfacial failure shown in Fig. 8b were examined, and the results are shown in Fig. 9a and b, respectively. It can be seen the weld area appeared uniform with some air bubbles as shown in Fig. 9a, and lack of fusion (i.e., unclosed gap) was observed in Fig. 9b. These results inferred that lack of fusion primarily was responsible for the weak strength and interfacial failure mode found in Fig. 8b. Therefore, it would be necessary to have a good part fit-up and high weld pressure to ensure the proper contacts at faying interface in single-sided ultrasonic welding.

3.5 Single-sided double pulse ultrasonic welding

From the aforementioned results, the poor contact between the workpieces was the main culprit for the discrepant welds. Referring to Figs. 5 and 7, both the overlap distance and gap between the workpieces influenced the contact between the

workpieces and the joint strength. Since the gap between the workpieces is inevitable for assembly in production, it would be desirable to develop a robust single-sided welding process.

In this study, a single-sided double-pulse ultrasonic welding (SSDPUW) shown in Fig. 10 is proposed. As shown, the process includes welding the fixed workpieces first, cooling the workpieces for a short period, and applying another ultrasonic vibration at substantially the same location on the existing weld. Extensive welding tests for SSUWed joints without gap between workpieces were performed with two different cooling times between the ultrasonic pulses, and the results are shown in Fig. 11. Referring to Fig. 11, a cooling time of 5-s was appropriate in terms of strength. This welding schedule was selected to assess the effect of gap on the strength of SSDPUW welds and the results are shown in Fig. 12. For the purpose of comparison, the strengths of the SSUW joints with various gaps between the workpieces are also included in Fig. 12. It can be seen that double-pulse vibration apparently minimized the negative impact

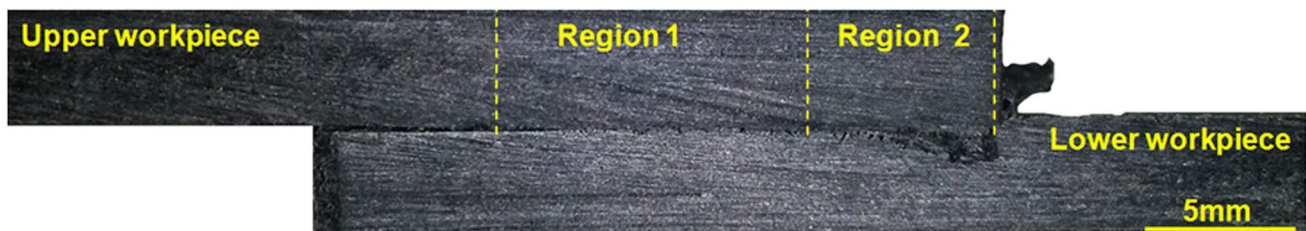
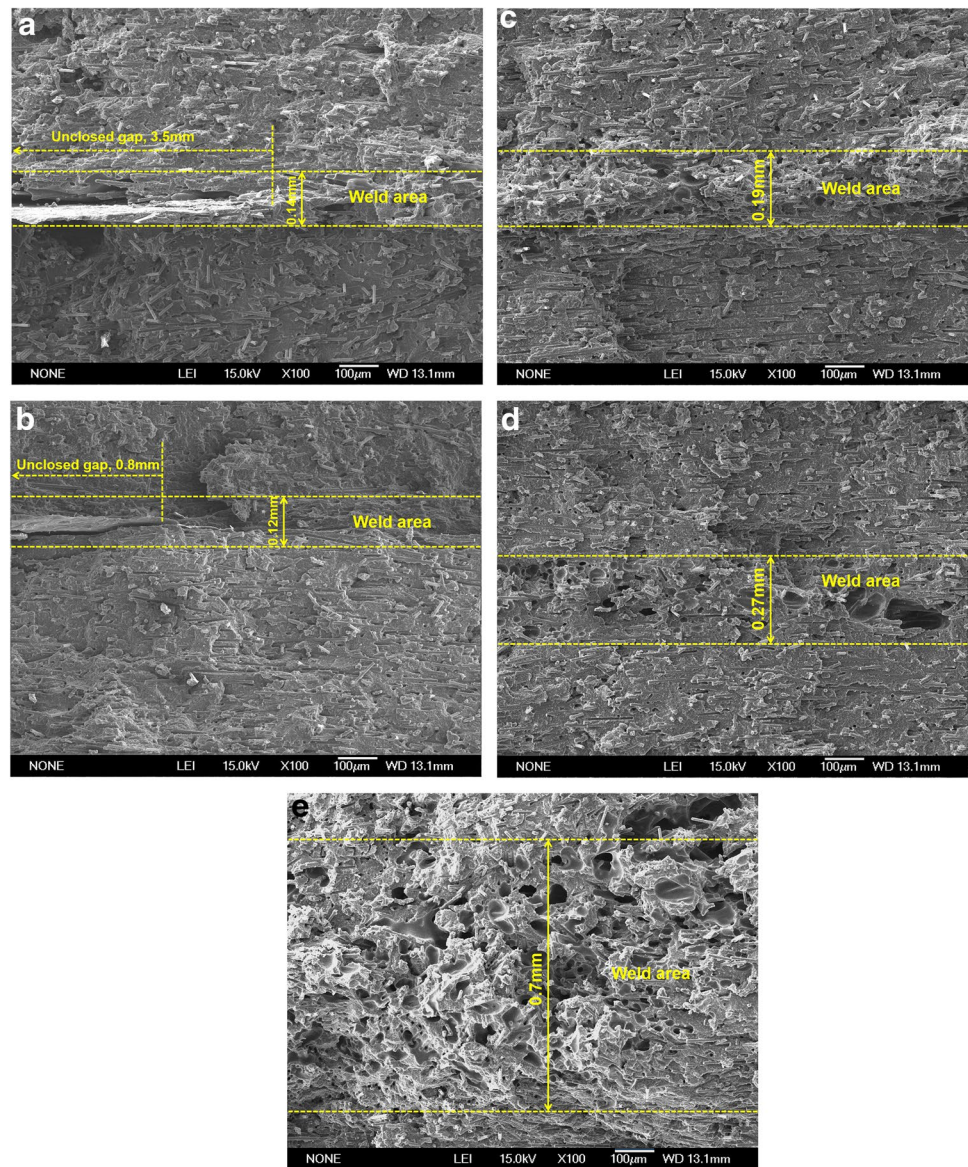


Fig. 15 Cross-section of the single-sided ultrasonic double-pulse welded carbon fiber/Nylon 66 composite with 30% mass fiber

Fig. 16 Effect of weld time of the second pulse on the microstructures at the region 1 of the SSDPUWed carbon fiber/Nylon 66 composite with a gap of 1.0 mm between the workpieces: **a** 0 s, **b** 0.5 s, **c** 0.9 s, **d** 1.3 s, and **e** 1.7 s



caused by the gap between the workpieces on the strength of the single-sided ultrasonic welded carbon fiber/Nylon 66 composite.

3.6 Joining mechanism of single-sided double pulse ultrasonic welding

To further understand the joining mechanism of SSUW of 4-mm-thick carbon fiber/Nylon 66 composite, the joints with a gap of 1.0 mm between the workpieces and an overlap distance of 40 mm were fabricated and mechanically tested. Figure 13 shows the effect of weld time of the second pulse on the strength and weld area of the SSDPUWed joints. For the purpose of comparison, the strength and weld area of the SSUW joints that were welded with a weld time of 1.3 s,

a weld pressure of 0.17 MPa, and overlap distance 40 mm are included in Fig. 13. The strengths of the SSDPUWed joints were comparable to that of the SSUW welds as the weld time of the second pulse exceeded 1.3 s. These results can be explained by the results shown in Fig. 14a to 14f in which the weld area increased with the weld time of the second pulse. Referring to Fig. 14a~f, the fusion area of the region 2 increased little with an increase in weld time of the second pulse while the fusion area of the region 1 increased significantly. Prolonging the weld time for the second pulse resulted in porous zone at fraying interface, and consequently resulted in a decrease in strength of the joints in spite of the large fusion area shown in Figs. 13 and 14. To examine further the evolution in microstructures of the SSDPUWed joints, the microstructure of the region 1

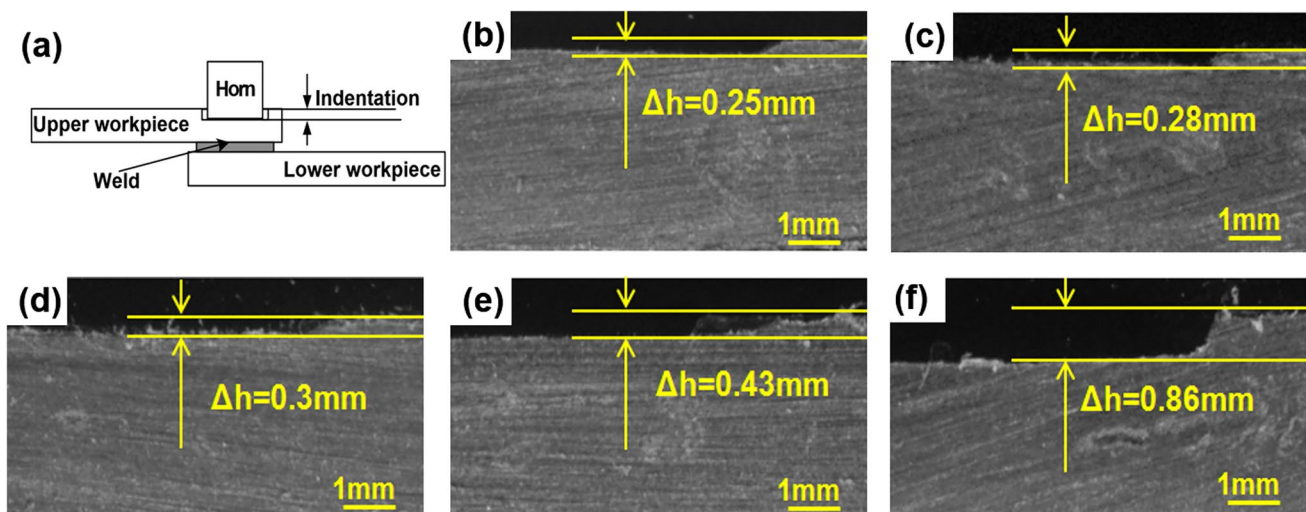


Fig. 17 Effect of weld time of the second pulse on the weld indentation of the SSDPUWed carbon fiber/Nylon 66 composite: **a** schematic of a weld indentation, **b** 0 s, **c** 0.5 s, **d** 0.9 s, **e** 1.3 s, and **f** 1.7 s

shown in Fig. 15 was analyzed. Figure 16a to e show the microstructures at the region 1 of the SSDPUWed welds made with the weld time of 0, 0.5, 0.9, 1.3, and 1.7 s, respectively. Referring to Fig. 16, the fusion zone grew with an increase in weld time of the second pulse. The fusion zone not only thickened but also contained significant porosity as the joints were welded with a weld time of 1.7 s. These results suggested that the materials became molten during the second ultrasonic pulse. The prolonged weld time raised the temperature, and thus degraded Nylon 66 during the second pulse [9, 26, 27].

3.7 Effect of double pulse vibration on decorative quality

The surface appearance of the welded joints is an important attribute for automotive applications. Since the second vibration pulse is applied, the decorative quality of the workpieces is a concern. To evaluate the effect of double-pulse vibration on the decorative quality, the upper workpieces of the welded joints were sectioned and the weld indentations were measured. Figure 17 presents the weld indentation of the SSDPUWed joints (with 1.0-mm gap between workpieces) made with various weld time of the second pulse. As shown, while the weld indentation increased little with the weld times less than 0.9 s, and then it increased quickly as the weld time prolonged. These results indicated that more energy was absorbed at horn-to-workpiece interface and the horn indented into the upper workpiece under a given weld pressure during the second pulse. To obtain the solid joint

strength and surface quality, it is recommended to select the proper weld time for single-sided double-pulse ultrasonic welding.

3.8 Significance of single-sided double-pulse ultrasonic welding of carbon fiber/Nylon 66

It is emphasized that the results presented in this study only illustrate the single-sided double pulse ultrasonic welding of 4-mm-thick carbon fiber composite with 30% mass fiber without energy director. The horn, part tolerance, and clamping conditions reported here are not indicative of conditions in vehicle assembly plants. Furthermore, design-of-experiment is needed to optimize the weld schedule to improve the weld quality. Nevertheless, the present results indicated that the application of double-pulse ultrasonic vibration not only improved the strength but also decreased the scatter in strength of the ultrasonic welds. Therefore, the process developed here can be considered as a potential method for single-sided ultrasonic welding of sheet-to-closed form thermoplastic composites. This study improves the robustness of the single-sided ultrasonic welding process and increases the flexibility of product designs that rely on the ultrasonic welding process for assembly.

4 Conclusions

Extensive tests conducted on single-sided ultrasonic welding of 4-mm-thick lapped carbon fiber/Nylon 66 composite with 30% mass fiber concluded the following:

1. The strength of the SSUWed joint made with proper selection of weld variables is comparable or even higher to that of the UWed joint.
2. The increased overlap distance had a negative effect on the strength of the SSUWed joint, and the strength is closely related with the weld area of region 1.
3. The existence of gaps between workpieces would decrease the strengths of SSUWed and UWed joints. However, it is feasible to obtain a solid weld with the use of double-pulse ultrasonic vibration schedule for the joint with gaps less than 1.0 mm.
4. The main mechanism of single-sided double-pulse ultrasonic welding of 4-mm-thick carbon fiber/Nylon 66 composite was the increase in weld area caused by the melting of the materials at periphery of the existing weld.

Funding This work was financially supported by the Natural Science Foundation of China (grant No. 51905167), Natural Science Foundation of Hunan Province (grant No. 2020JJ5197, 2019JJ50181), Hunan Provincial Department of Education Project (19C0760), and GM-Research and Development.

References

1. Kumar HGP, Xavier MA (2021) Composite materials production for automobile applications. *Ref Mod Mater Sci Mater Eng* 2021. <https://doi.org/10.1016/B978-0-12-803581-8.11894-6>
2. Godara SS, Nagar SN (2020) Analysis of frontal bumper beam of automobile vehicle by using carbon fiber composite material. *Mater Today Proc* 26:2601–2607. <https://doi.org/10.1016/j.matpr.2020.02.550>
3. Park G, Park H (2018) Structural design and test of automobile bonnet with natural flax composite through impact damage analysis. *Compos Struct* 184:800–806. <https://doi.org/10.1016/j.compsstruct.2017.10.068>
4. Witik RA, Payet J, Michaud V, Ludwig C, Manson JAE (2011) Assessing the life cycle costs and environmental performance of lightweight materials in automobile applications. *Compos Part A* 42:1694–1709. <https://doi.org/10.1016/j.compositesa.2011.07.024>
5. Gu F, Hall P, Miles NJ (2016) Development of composites based on recycled polypropylene for injection moulding automobile parts using hierarchical clustering analysis and principal component estimate. *J Clean Prod* 137:623–643. <https://doi.org/10.1016/j.jclepro.2016.07.028>
6. Zhang GP, Li JC, Liu ZX, Wang PC (2020) Application of ultrasonic welding to repair adhesively bonded short carbon fiber reinforced Nylon 6 composites. *Int J Adhes Adhes* 100:102603. <https://doi.org/10.1016/j.ijadhadh.2020.102603>
7. Chinnadurai T, Saravanan S, Prabaharan N, Pandian MK, Deebika S (2018) Analyzing the weld strength of ultrasonic polymer welding using artificial neural networks. *Mater Today Proc* 5:28320–28327. <https://doi.org/10.1016/j.matpr.2018.10.116>
8. Li H, Cao B (2019) Effects of welding pressure on high-power ultrasonic spot welding of Cu/Al dissimilar metals. *J Manuf Process* 40:194–203. <https://doi.org/10.1016/j.jmapro.2019.07.018>
9. Zhi Q, Tan XR, Lu L, Chen LY, Li JC, Liu ZX (2017) Decomposition of ultrasonically welded carbon fiber/polyamide 66 and its effect on weld quality. *Weld World* 61:1017–1028. <https://doi.org/10.1007/s40194-017-0482-5>
10. Gu XY, Sui CL, Liu J, Li DL, Meng ZY, Zhu KX (2019) Microstructure and mechanical properties of Mg/Al joints welded by ultrasonic spot welding with Zn interlayer. *Mater Des* 181:108103. <https://doi.org/10.1016/j.matdes.2019.108103>
11. Parmar U, Pandya DH (2016) Experimental investigation of ultrasonic welding on non-metallic material. *Procedia Technol* 23:551–557. <https://doi.org/10.1016/j.protcy.2016.03.062>
12. Jongbloed B, Teuwen JL, Benedictus R, Villegas IF (2020) On differences and similarities between static and continuous ultrasonic welding of thermoplastic composites. *Compos Part B Eng* 203:108466. <https://doi.org/10.1016/j.compositesb.2020.108466>
13. Levy A, Poitou A, Corre SL, Soccard E (2008) Ultrasonic welding of thermoplastic composites, modeling of the process. *Int J Mater Form* 1:887–890. <https://doi.org/10.1007/s12289-008-0238-2>
14. Zhao T, Broek C, Palardy G, Villegas IF, Benedictus R (2018) Towards robust sequential ultrasonic spot welding of thermoplastic composites: welding process control strategy for consistent weld quality. *Compos A Appl* 109:335–367. <https://doi.org/10.1016/j.compositesa.2018.03.024>
15. Benatar A, Gutowski GT (1989) Ultrasonic welding of PEEK graphite APC-2 composites. *Polym Eng Sci* 29:1705–1721. <https://doi.org/10.1002/pen.760292313>
16. Villegas IF, Bersee HEN (2010) Ultrasonic welding of advanced thermoplastic composites: an investigation on energy-directing surfaces. *Adv Polym Tech* 29:112–121. <https://doi.org/10.1002/adv.20178>
17. Tao W, Su X, Wang HH, Zhang ZH, Li H, Chen J (2019) Influence mechanism of welding time and energy director to the thermoplastic composite joints by ultrasonic welding. *J Manuf Process* 37:196–202. <https://doi.org/10.1016/j.jmapro.2018.11.002>
18. Levy A, Corre SL, Villegas IF (2014) Modeling of the heating phenomena in ultrasonic welding of thermoplastic composites with flat energy directors. *J Mater Process Technol* 214:1361–1371. <https://doi.org/10.1016/j.jmatprotec.2014.02.009>
19. Li Y, Yu B, Wang BC, Lee TH, Banu M (2020) Online quality inspection of ultrasonic composite welding by combining artificial intelligence technologies with welding process signatures. *Mater Des* 194:108912. <https://doi.org/10.1016/j.matdes.2020.108912>
20. Weglowska A, Pietras A (2012) Influence of the welding parameters on the structure and mechanical properties of vibration welded joints of dissimilar grades of nylons. *Arch Civ Mech Eng* 12:198–204. <https://doi.org/10.1016/j.acme.2012.03.009>
21. Zhi Q, Lu L, Liu ZX, Wang PC (2018) Influence of horn misalignment on weld quality in ultrasonic welding of carbon fiber polyamide 66 composite. *Weld J* 97:133s–143s. <https://doi.org/10.29391/2018.97.012>
22. Chung YM, Kamal MR (2008) Morphology of PA-6 vibration welded joints and its effect on weld strength. *Polym Eng Sci* 48:240–248. <https://doi.org/10.1002/pen.20830>
23. Bates PJ, MacDonald J, Sidiropoulos V, Kontopoulou M (2005) Comparison of experimental and analytical vibration welding meltdown-time profiles for nylon 66 and polypropylene. *Polym Eng Sci* 45:798–797. <https://doi.org/10.1002/pen.20333>
24. Zhi Q, Gao YH, Lu L, Liu ZX, Wang PC (2018) Online inspection of weld quality in ultrasonic welding of carbon fiber/

- polyamide 66 without energy directors. *Weld J* 97:65s-74s. <https://doi.org/10.29391/2018.97.006>
25. Matsuoka S (1995) Ultrasonic welding and characteristics of glass-fiber reinforced plastic: comparison between the paper-making method and the impregnation method. *J Mater Process Technol* 55:427–431. [https://doi.org/10.1016/0924-0136\(96\)83108-6](https://doi.org/10.1016/0924-0136(96)83108-6)
26. Jia F, Mao JL, Yang XY, Ma Y, Yao C (2013) Thermal, physical and mechanical properties of hydrogenated dimer acid-based Nylon 636/Nylon 66 copolymers. *Chin Chem Lett* 24:654–658. <https://doi.org/10.1016/j.ccl.2013.04.012>
27. Wang KF, Li Y, Banu M, Li JJ, Guo WH, Khan H (2017) Effect of interfacial preheating on welded joints during ultrasonic composite welding. *J Mater Process Technol* 246:116–122. <https://doi.org/10.1016/j.jmatprotec.2017.03.014>

Publisher's note Springer Nature remains neutral with regard to jurisdictional claims in published maps and institutional affiliations.